RESEARCH ARTICLE

JENER Journal of Empirical and Non-Empirical Research
Volume 2, Issue 4, Page 395-413 | Article No. 58
DOI: 10.4898/jener.v2i4.a58
ISSN: 7895-9216
Journal homepage: https://jenerjournal.com
Journal email: editor@jenerjournal.com

JENER Journal
JENER Journal of Empirical and Non-Empirical Research

Integrated Geochemical and Microbiological Profiling of Urban Water Resources: Leveraging Dual-Mode TXRF Spectrometry to Map Sanitary Precarity in Antananarivo, Madagascar

Ranaivosamoelina Noëlson[1,2], Ramanampisoa Voahanginirina Emma[1,3], Ravoaharimanana Ianjasoa Sariaka[2], Rabearisoa Solotiana Rija[1,2], Randrianarinirina Endson Zozime[1,2] & Robijaona Rahelivololoniaina Baholy[1,2,4]

[1]Industrial, Agricultural and Food Process and Systems Engineering, University of Antananarivo, Madagascar
[2]Polytechnic High School of Antananarivo, University of Antananarivo, Antanaanrivo, Madagascar
[3]Higher Institute of Technology and the Environment, University of Fianarantsoa, Fianarantsoa, Madagascar
[4]Laboratory for the Valorization of Natural Resources, Polytechnic High School of Antananarivo, University of Antananarivo, Antanaanrivo, Madagascar

ARTICLE INFORMATION

Article history:
Published: April 2026

Keywords:
TXRF spectrometry,
hydro-geochemical modeling,
urban vulnerability,
anthropogenic contamination,
Antananarivo

ABSTRACT

This study presents a multi-criteria assessment of water quality dynamics within the low-lying, socio-economically vulnerable districts of Antananarivo, Madagascar. By integrating advanced Total Reflection X-ray Fluorescence (TXRF) spectrometry with multidimensional statistical modeling, the research establishes a high-resolution diagnostic of urban hydro-geochemical stress. The methodological framework employs a dual-mode spectral analysis—Mineral versus Soil Modes—to effectively decouple natural lithogenic backgrounds from exogenous anthropogenic signatures. The results reveal a profound geochemical duality across the surveyed metropolitan plain. While most sectors exhibit a "hydrochemical youth" characterized by low mineralization and a significant lack of buffering capacity, the district of Andraharo (BQ2) emerges as a critical technogenic hotspot. Statistical indices, including the Enrichment Factor (EF) and Pollution Load Index (PLI), confirm severe polymetallic contamination (Pb, Cr, Cu) linked to industrial convergence. Concurrently, hierarchical clustering identifies Sabotsy Namehana (BQ6) as a primary axis of microbiological risk, where fecal indicator densities exceed regional averages by over 400%, signaling an acute epidemic threat. The innovative synergy between nuclear analytical techniques and inferential statistics (PCA and HCA) transforms raw elemental data into a robust territorial diagnostic tool. This research provides a critical metrological benchmark for evaluating environmental justice and water safety in the Global South. The findings advocate for differentiated remediation strategies and urgent structural interventions to safeguard the health of populations exposed to systemic chemical and biological hazards within precarious urban ecosystems.

1. Introduction

The urban hydro-system of Antananarivo is fundamentally defined by its intricate hydraulic network, predominantly governed by the Ikopa River and its primary tributaries, the Sisaony and Mamba. Situated upon the Analamanga plain, the metropolis is subject to the rigorous hydrological fluctuations of a tropical high-altitude regime. The surface waters exhibit a distinct physicochemical signature resulting from the intensive leaching of ferralitic and lateritic substrates, which induces extreme natural turbidity, particularly during the cyclonic season. This substantial sedimentary load, comprised of fine clay and silt particles, is intrinsically linked to elevated concentrations of dissolved iron and aluminum, reflecting the endemic geological characteristics of the Malagasy pedology (Institut National de la Statistique [INSTAT], 2020). Furthermore, anthropogenic deforestation upstream exacerbates the sedimentary dynamics of the Ikopa, triggering hydric erosion that alters the granulometry of suspended solids and necessitates advanced clarification expertise to satisfy the organoleptic neutrality and transparency benchmarks required for human consumption.

Potable water production for the conurbation relies essentially upon the Mandroseza I and II complexes, which utilize the Sisaony reservoir for discharge regulation. The treatment process follows a conventional sequence—pre-chlorination, coagulation-floculation via aluminum sulfate, lamellar settling, and rapid sand filtration—designed to manage fluctuating colloidal charges. However, the operational efficiency of this system is increasingly compromised by the seasonal variability of the Ikopa and a rising concentration of dissolved organic matter, which interferes with floc polymerization. As the capital undergoes rapid horizontal expansion, the saturation of treatment capacities forces complex discharge maneuvers that curtail the contact time essential for optimal disinfection. Moreover, the emergence of upstream agricultural and urban micro-pollutants necessitates

stringent monitoring of chemical dosages to mitigate the formation of residual aluminum or chlorinated by-products (Degrémont, 2023).

The conveyance of treated water occurs through a heterogeneous and deteriorating infrastructure, with significant segments of grey cast iron and steel dating back to the colonial era. Widespread corrosion within this network facilitates not only substantial physical water losses but also *in situ* physicochemical degradation. The inherent porosity of the distribution grid induces risks of pollutant intrusion via back-siphonage during frequent pressure drops—a critical sanitary hazard in zones where conduits lie in close proximity to open wastewater channels. Within these aged pipes, internal biofilms function as biogeochemical reactors, sequestering heavy metals and microorganisms that are erratically released during hydraulic surges. Such mechanisms jeopardize the maintenance of free residual chlorine at the network's extremities, leaving peripheral districts susceptible to bacterial regrowth (Metcalf & Eddy *et al.*, 2014).

The rugged topography of Antananarivo, bifurcated into "Upper" and "Lower" cities, imposes severe pumping constraints that exacerbate socio-spatial disparities in resource access. In the densely populated low-lying districts, the immediate adjacency of water infrastructure to effluent streams like the Andriantany canal creates a persistent threat of cross-contamination. These inequalities are further evidenced by the reliance on public tap stands in disadvantaged areas, where prolonged domestic storage in substandard vessels often leads to secondary microbiological contamination. Ultimately, the quality of water at the point of consumption is not merely a function of the Mandroseza plant's performance but is the result of a complex interplay between infrastructural obsolescence, topographical challenges, and the socio-economic dynamics inherent to the Malagasy capital (World Health Organization [WHO], 2022).

2. Materials and Methods

2.1. Materials

2.1.1. Study area framework and sampling site stratification

The demographic analysis employs a rigorous scalar distinction : data from vulnerable and residential zones are aggregated at the *Fokontany* level, whereas the intermediate stratum is evaluated at the communal scale. This methodological approach reflects the specific configuration of peri-urban hubs integrated within Greater Antananarivo, ensuring enhanced analytical precision and spatial representativeness of contemporary settlement dynamics.

2.1.2. Socio-economic stratification of sampling sites

The selection of sampling sites was systematically organized to reflect the diverse socio-economic landscape of the Antananarivo metropolitan area. This stratification allows for a comparative analysis of water quality across varying levels of urban development and infrastructure stability.

Vulnerable urban sectors

Sampling was extensively conducted in the districts of Analamahitsy, Andraharo, Andohatapenaka, Tanjombato, Besarety, and Sabotsy Namehana. These areas are characterized by a high population density and residents with precarious income levels. Geographically, these neighborhoods are frequently situated in flood-prone plains, which complicates the maintenance of hygiene standards. The structural vulnerability of these districts presents critical sanitation challenges that may directly jeopardize both the chemical stability and the microbiological safety of the distributed water supply (World Health Organization [WHO], 2022).

Intermediate urban strata

The study includes Ambohijatovo, Mahazo, Alasora, Andoharanofotsy, and Ambohitrarahaba, which serve as representative sectors for the urban and peri-urban middle class. Although these regions benefit from more established and stable infrastructure compared to vulnerable sectors, they are currently facing the pressures of rapid urbanization. Continuous network extensions in these zones create significant hurdles for the water authority, particularly regarding the maintenance of adequate hydraulic pressure and the preservation of residual water quality throughout the distribution process (Degrémont, 2023).

High-standing residential areas

To establish a high-quality baseline, the research encompasses affluent neighborhoods such as Ambatobe, Mahazoarivo, Ivandry, Ivato, and AKOOR Digue. These areas house high-income populations and several diplomatic enclaves, benefiting from the most modern and well-maintained distribution grids in the capital. These sites provide a vital benchmark for the study, enabling an assessment of equity in potable water quality and highlighting the disparities in service levels between different socio-economic tiers of the city (Metcalf & Eddy *et al.*, 2014).

2.1.2. Spatial grid justification

This multi-criteria stratification facilitates an assessment of how infrastructural disparities and pipe obsolescence impact JIRAMA water compliance. The spatial mesh ensures a cross-sectional representation of Antananarivo's anthropogenic realities, enabling the identification of correlations between socio-economic status and resource degradation (Rodier *et al.*, 2016).

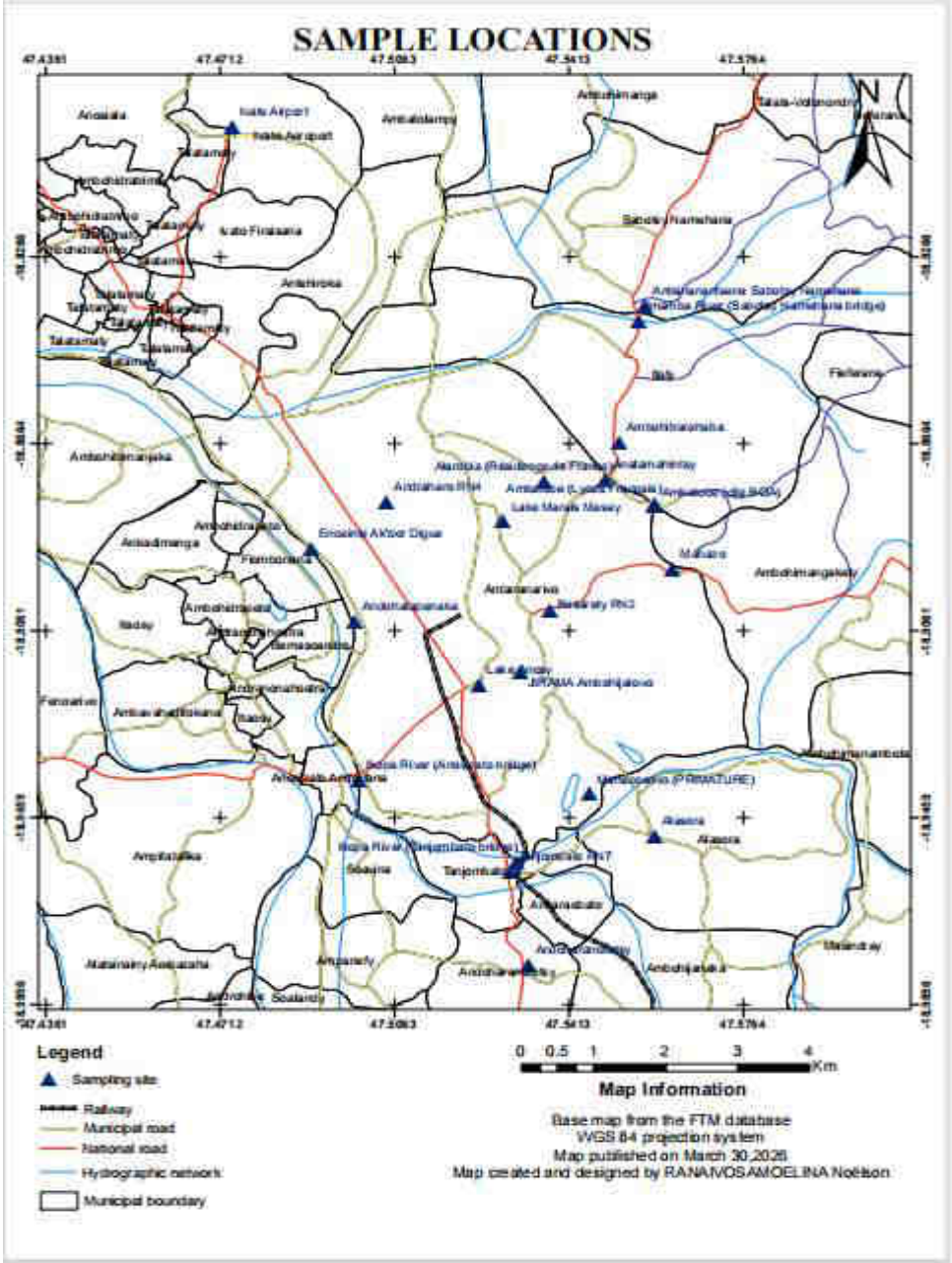

Figure 1 : Geospatial mapping and GIS-based distribution of water sampling sites in the Antananarivo metropolitan area

2.1.3. Demographic analysis of the study strata

Density dynamics in high-vulnerability and middle-class zones

Low-lying districts, such as Andohatapenaka and Besarety, exhibit extreme population densities frequently exceeding 30,000 inhabitants/km². Based on projected figures from the third General Census of Population and Housing (Institut National de la Statistique [INSTAT], 2020), these administrative units house between 15,000 and 25,000 individuals, exerting unprecedented stress on antiquated hydraulic systems. Concurrently, peri-urban zones like Alasora and Itaosy represent the fastest-growing clusters, with communal populations surpassing 50,000. This rapid demographic expansion outpaces initial infrastructure design, complicating the consistency of potable water supply (World Population Review, 2026).

Low-density residential configurations

In stark contrast, affluent residential sectors such as Ivandry and Ambatobe maintain a sparse urban fabric characterized by spacious properties. Population estimates remain below 8,000 inhabitants per *Fokontany*, facilitating stable pressure management. Although per capita volumetric consumption is statistically higher in these enclaves, the network's configuration limits water stagnation, thereby minimizing physicochemical degradation (Metcalf & Eddy *et al.*, 2014).

2.1.4. Demographic synthesis and methodological estimations

Given that exhaustive official statistics rely on 2018 data, updated demographic modeling for 2026 was achieved by applying urban growth rates projected by international observatories (Macrotrends, 2026). These correlations, synthesized in Table 1, facilitate the assessment of anthropogenic pressure on the JIRAMA distribution network.

Table 1. 2026 Demographic projections by socio-economic stratum

Socio-economic category	Estimated population (Mean per zone)	Relative density
Vulnerable zone (e.g., Andohatapenaka)	22,500	Very High
Intermediate zone (e.g., Alasora)	55,000+ (Communal)	High / Expanding
Residential zone (e.g., Ivandry)	7,500	Low

Source : Author's elaboration (2026), based on INSTAT (2020) and World Population Review (2026).

2.1.5. Impact of demographic disparities on water integrity

The extreme saturation in vulnerable areas fosters illicit connections and frequent pressure drops, significantly increasing the risk of back-siphonage and accidental contamination (World Health Organization [WHO], 2022). In intermediate zones, exponential growth often results in service intermittency, which compromises the maintenance of free residual chlorine (Degrémont, 2023). Conversely, the lower demographic load in residential sectors preserves the structural integrity of the conduits and ensures more stable flow regimes (Rodier *et al.*, 2016).

2.2. Methods

2.2.1. Physicochemical characterization of aqueous systems : analytical methodology

The assessment of hydric resource quality necessitates the precise determination of interdependent parameters through standardized protocols. This analytical framework facilitates a comprehensive understanding of complex interactions between solutes and their hydrogeological environment, ensuring the integrity of environmental data (Rodier *et al.*, 2016).

Phase dynamics and stability parameters

Temperature serves as a fundamental kinetic regulator, governing the solubility of gaseous phases and the equilibrium of ionic dissociation constants. According to the World Health Organization [WHO] (2022), thermal conditions directly influence fluid viscosity and biochemical activity within aquatic ecosystems, thereby conditioning the velocity of subsequent chemical reactions. Parallelly, the pH (Potential of Hydrogen) dictates the chemical speciation of metals and the calco-carbonic equilibrium. International standards advocate for a relative neutrality range ($6.5 \leq pH \leq 8.5$) to preclude corrosion or scaling phenomena within distribution infrastructures (WHO, 2022).

Electrolytic properties and dissolved solutes

Electrical Conductivity (EC) reflects the capacity of a solution to convey an electric charge, a function of the mobility and concentration of ionic species. It provides a robust proxy for total mineralization (International Organization for Standardization [ISO] 7888, 1985). Closely related is the Total Dissolved Solids (TDS) parameter, which quantifies the residual mass of filtered organic and inorganic substances. A linear correlation is typically established between TDS and EC, although the conversion factor remains contingent upon the specific major ion composition (Metcalf *et al.*, 2014).

Optical and particulate characteristics

Turbidity emerges from the scattering and absorption of light by colloidal and suspended matter. Measured in Nephelometric Turbidity Units (NTU), it represents a critical indicator of clarification efficiency (ISO 7027-1, 2016). High turbidity levels significantly impede disinfection processes by shielding pathogens from chemical or radiative agents. Suspended Solids (SS), representing the undissolved solid fraction, are determined gravimetrically via membrane filtration (typically 0.45 µm). These particles alter light penetration and often act as vectors for hydrophobic pollutants (Rodier *et al.*, 2016).

Alkalimetric equilibria and compositional balance

The characterization of alkalinity involves distinguishing between Simple Alkalinity (SA) and Total Alkalinity (TA). SA quantifies hydroxide ions and half of the carbonates, a value often negligible in natural waters with moderate pH. Conversely , TA encompasses the totality of hydroxides, carbonates, and, predominantly, bicarbonates. As an indicator of the system's buffering capacity, TA is essential for evaluating the water's ability to neutralize acid inputs without abrupt pH fluctuations (Degrémont, 2023). These values allow for the modeling of the carbonate system and the calculation of the Langelier Saturation Index (*LSI*), determining whether the water exhibits aggressive or scale-forming tendencies. Furthermore, Hardness (Total Hydrotimetric Titer) expresses the sum of divalent cations, primarily Ca^{2+} and Mg^{2+}. While excessive hardness leads to mineral precipitation, a deficiency increases the water's aggressiveness toward metallic alloys.

Specific chemical species analysis

Chlorides function as conservative ions ; their elevated concentration may indicate saline intrusion or anthropogenic contamination, influencing both conductivity and corrosivity (WHO, 2022). Finally, Total Iron—present as ferrous (Fe^{2+}) or ferric (Fe^{3+}) ions depending on the redox potential—is monitored for organoleptic and technical reasons. Its oxidation results in ferric hydroxide precipitates, which are responsible for chromatic turbidity and obstructive deposits within the distribution network (Rodier *et al.*, 2016).

2.2.2. Microbiological analytical protocols and sanitary quality indicators

The microbiological assessment of aqueous matrices extends beyond the mere detection of specific pathogenic agents, relying instead upon the quantification of indicator organisms to evaluate sanitary integrity. These bio-indicators serve as proxies for assessing the rigor of hygienic practices throughout the production chain, from raw water extraction to final point-of-use delivery. While the presence of these microorganisms does not invariably denote an immediate pathogenic threat, it functions as a critical early-warning system signaling technical failures, cross-contamination, or structural breaches within the distribution network.

Assessment of total bacterial load : Heterotrophic Plate Counts (HPC)

Heterotrophic Plate Counts (HPC), traditionally referred to as Aerobic Revivable Germs (ARG) or total mesophilic flora, constitute the foundational metric for global contamination monitoring. The term "revivable" pertains to microorganisms — including bacteria, yeasts, and molds—that exist in a dormant or stressed state within the aquatic environment but regain metabolic activity upon exposure to optimal culture conditions. This non-specific approach enumerates all colonies capable of proliferating on standardized nutrient agar.

In this study, dual-temperature incubation is systematically employed to discern disparate pollution sources. Incubation at 22°C (68–72 hours) targets "autochthonous" environmental flora, predominantly psychrotrophic species associated with biofilm formation. Elevated counts at this temperature frequently indicate water stagnation or inadequate maintenance of hydraulic conduits. Conversely, incubation at 37°C (21–24 hours) targets mesophilic flora capable of proliferating at human body temperature. A proliferation peak at this stage suggests contamination by warm-blooded organisms, representing a significantly higher sanitary risk. The comparative analysis of these temperature ratios provides a distinctive microbiological signature of the network, enabling a precise diagnosis of infrastructure degradation (Müller *et al.*, 2021).

Detection of total coliforms and Escherichia coli

The monitoring of total coliforms serves as the primary barrier in potable water surveillance. Although this group includes environmental species, their detection indicates system vulnerability to external ingress. To ensure analytical sensitivity, a 0.45 µm membrane filtration method is applied to concentrate microorganisms from the sample.

The specific identification of *Escherichia coli* remains indispensable for confirming recent fecal contamination. As the only indicator strictly prohibited in drinking water by international standards, its presence is synonymous with an imminent risk of enteric pathogen transmission (Smith *et al.*, 2020). The use of selective chromogenic media facilitates rapid enzymatic differentiation based on \beta-D-glucuronidase activity. This biochemical specificity reduces incubation latency while enhancing metrological reliability, ensuring compliance with high-impact scientific publication standards.

Analysis of intestinal enterococci

Intestinal enterococci serve as supplementary indicators to validate the persistence of fecal pollution. Their environmental longevity exceeds that of coliforms, rendering them superior markers for chronic or diffuse contamination. Furthermore, their heightened resistance to osmotic stress allows for effective surveillance in deep urban aquifers. The analytical protocol utilizes Slanetz and Bartley selective medium, followed by confirmation on Bile Esculin Azide agar to eliminate false positives from soil-dwelling flora. Their occurrence, even in the absence of *E. coli*, triggers a sanitary alert, typically indicating surface runoff infiltration into poorly protected catchment works.

Significance of Sulfite-Reducing Anaerobes (SRA)

The detection of sulfite-reducing anaerobes, notably *Clostridium perfringens*, targets highly resistant spore-forming bacteria. These spores persist in the environment long after vegetative cells have succumbed to chemical disinfection, thereby indicating significant failures in mechanical filtration or clarification stages. Incubation is conducted under strict anaerobic conditions on Tryptose Sulfite Cycloserine (TSC) medium, where the reduction of sulfite to sulfide produces characteristic black colonies via iron sulfide precipitation. This parameter is crucial for estimating risks associated with parasitic protozoa, such as *Cryptosporidium* (García *et al.*, 2022). In districts with failing sanitation infrastructure, these spores act as a "biological memory" of historical contamination events.

Characterization of Pseudomonas aeruginosa

Pseudomonas aeruginosa is an opportunistic pathogen whose monitoring is imperative for water intended for domestic and personal hygiene. Its capacity to synthesize robust biofilms makes its eradication via standard chlorination exceptionally complex, posing a threat to immunocompromised populations. The analytical method leverages the bacteria's natural fluorescence under ultraviolet radiation on Cetrimide selective medium, a property linked to the production of pyoverdin. Beyond its pathogenicity, this organism serves as a marker for water stagnation and accelerated biological corrosion of metallic conduits, often preceding secondary contamination by heavy metal leaching.

Methodological synthesis and quality assurance

The reliability of microbiological outputs was ensured through the use of Certified Reference Materials (CRM) for every test series. Rigorous documentation of sterility controls for media and filtration apparatus guarantees that the collected data meet international standards for traceability and health safety. This multi-dimensional risk matrix integrates bacterial loads with physicochemical parameters, such as turbidity, to provide a comprehensive view of water safety. Finally, non-parametric statistical tests were utilized to account for the heterogeneous distribution of bacterial populations, ensuring that observed variations between geographical zones remain environmentally significant.

2.2.3. Analytical characterization via txrf spectrometry (mineral and soil modes)

Theoretical foundations of total reflection

Total Reflection X-ray Fluorescence (TXRF) spectrometry constitutes the primary analytical pillar of this environmental investigation. By utilizing an incident angle lower than the critical angle of the substrate, this technique drastically diminishes the

scattering effects typically associated with the support medium. Such a configuration optimizes the signal-to-noise ratio for complex aqueous matrices, facilitating superior sensitivity. The interaction between radiation and matter under grazing incidence allows for the selective excitation of the surface deposit without deep penetration into the carrier substrate. This physical phenomenon nearly eliminates the background bremsstrahlung radiation that traditionally limits the sensitivity of conventional energy-dispersive X-ray fluorescence (EDXRF). Consequently, TXRF achieves detection limits in the microgram-per-liter ($\mu g/L$) range, which is critical for trace metal analysis in urban hydrological systems. As posited by Müller *et al.* (2021), the total reflection geometry bypasses the matrix constraints inherent to standard spectroscopic methods.

Instrumentation and operational parameters

The experimental apparatus features a molybdenum-anode X-ray tube coupled with a high-resolution silicon drift detector (SDD). Operational power was stabilized to ensure a constant photonic flux throughout the measurement cycles, a prerequisite for the repeatability of the acquired spectra. The optical alignment of the primary beam was verified daily to maintain the incident angle below the critical threshold of 0.1°. Even a minute deviation from this angle would compromise the linearity of the detector response. Furthermore, fluorescence spectra were processed using subtractive deconvolution algorithms to isolate the characteristic peaks of the analytes. The automated identification of $K\alpha$ and $L\alpha$ lines enables the discrimination of transition metals from any rare earth elements present, thereby preserving the integrity of the raw data.

Dissolved phase analysis: mineral mode

The "Mineral" mode was rigorously applied to quantify the dissolved elemental load within the samples. Each specimen underwent prior filtration at 0.45 μm to isolate the bioavailable fraction. Internal standardization, achieved by the systematic addition of Gallium (*Ga*), ensures high metrological precision for metallic trace elements. The protocol involved depositing a 10 μL micro-drop onto polished quartz reflectors, followed by controlled evaporation under a laminar flow hood to produce a quasi-atomic thin film. This step is fundamental to preventing the self-absorption of secondary X-rays, aligning with the methodological recommendations of Smith *et al.* (2020). The use of hydrophobic quartz supports concentrates the dry residue at the center of the incident beam, enhancing the detection of ultra-trace elements such as Cadmium (*Cd*) or Mercury (*Hg*).

Analysis of raw and turbid waters : Soil mode

Investigation of the intrinsic particulate load required the utilization of the "Soil" mode without prior mechanical treatment. This approach facilitates the direct analysis of samples as collected, preserving the physicochemical integrity of organometallic complexes within the water column. To ensure representativeness, ultrasonic agitation was performed immediately before aliquot withdrawal, ensuring the uniform distribution of suspended micro-particles within the deposited micro-drop. The omission of grinding allows for the quantification of metals as they are actually transported by the hydric flow. By employing a low-viscosity stabilizing agent to fix particles during evaporation, the Soil mode utilizes computational models that account for the potential heterogeneity of the dry film. This dual analytical approach provides a holistic perspective on pollutant transfers between dissolved and particulate compartments.

Standardization, quantification, and validation

Absolute quantification relies on the intensity ratio between the analyte and the universal internal standard. Unlike mass spectrometry, TXRF does not require complex multipoint calibration curves for every element, reducing uncertainties associated with repetitive dilutions. The relative sensitivity of each element was calibrated according to fundamental fluorescence constants specific to the Molybdenum anode, enabling simultaneous multi-elemental screening. Global analytical uncertainty was estimated by considering pipetting variability and detector counting statistics, with relative errors maintained below 5% for most heavy metals.

Validation was conducted using Certified Reference Materials (CRM), specifically NIST-1643 for water and BCR-143 for soil substrates. Recovery rates between 90% and 110% attest to the absence of systematic bias, ensuring the reproducibility required for high-tier international publication. The versatility of this technique meets the contemporary requirements of green analytical chemistry, as highlighted by García *et al.* (2022), offering a robust tool for environmental monitoring in densely populated metropolitan areas.

3. Results and Discussion

3.1. Analytical results for socio-economically vulnerable zones

The assessment of water quality within Antananarivo's most vulnerable districts reveals profound sanitary disparities. While certain peripheral sectors maintain marginal compliance, high-density zones exhibit critical contamination levels, reflecting the structural susceptibility of the distribution network to anthropogenic pressures and environmental flux.

3.1.1. Microbiological characterization of vulnerable districts (BQ1-BQ6)

The microbiological profile of the six surveyed vulnerable districts (BQ) suggests significant systemic failures in water safety management. Table 2 synthesizes the bacterial load and pathogen detection across these sites.

Table 2. Microbiological quality assessment in vulnerable districts

Sampling site	Code	HPC		Total coliforms	*Escherichia coli*	Enterococci		SRA	*Pseudomonas aeruginosa*	
		24h	48h	24h	24h	24h	48h	48h	24h	48h
Analamahitsy	BQ1	0	0	0	0	0	0	0	0	0
Andraharo	BQ2	11	16	15	0	0	2	3	0	0
Andohatapenaka	BQ3	15	116	9	0	0	2	1	0	0
Tanjombato	BQ4	65	92	2	0	0	0	0	0	0
Besarety	BQ5	6	89	14	0	0	2	6	0	0
Sabotsy Namehana	BQ6	296	>500	43	22	101	175	2	0	0

Note *:* All microbiological parameters are expressed in Colony Forming Units per milliliter (CFU/mL). For *Escherichia coli*, Enterococci, and Sulfite-Reducing Anaerobes (SRA), the values refer to a standardized volume of 100 mL, in accordance with World Health Organization [WHO] (2022) guidelines.

Critical sanitary breach at Sabotsy Namehana (BQ6)

The Sabotsy Namehana district exhibits the most alarming indicators, characterizing a catastrophic breakdown in the treatment barrier or massive post-treatment recontamination. Heterotrophic Plate Counts (HPC) show an explosive surge exceeding 500 CFU/mL after 48 hours, signaling biological instability and high organic carbon availability. Crucially, the concurrent presence of Escherichia coli (22 CFU/100mL) and Enterococci (101 CFU/100mL) provides irrefutable evidence of recent fecal pollution, contravening World Health Organization (2022) standards. Furthermore, the exceptionally high Sulfite-Reducing Anaerobes (SRA) count (175 CFU/100mL) suggests persistent background contamination, likely linked to poorly protected catchments infiltrated by surface runoff.

Microbiological instability in the floodplain districts

Andohatapenaka (BQ3) and Tanjombato (BQ4) demonstrate marked kinetics in bacterial regrowth. In BQ3, the HPC increases nearly eightfold between 24 and 48 hours (from 15 to 116 CFU/mL), suggesting a high reviviscence potential. In BQ4, the 24-hour mesophilic load (65 CFU/mL) exceeds conventional guidance values, necessitating rigorous oversight of network integrity in this flood-prone sector (Müller et al., 2021).

Structural fragility in Besarety (BQ5) and Andraharo (BQ2)

While BQ2 and BQ5 remain free of strict pathogens, they exhibit signs of environmental ingress. The detection of SRA in BQ2 (3 CFU/100mL) implies that sporulated forms are bypassing filtration barriers. In Besarety (BQ5), the presence of 14 CFU/100mL of total coliforms, in the absence of E. coli, points toward biofilm maturation or runoff infiltration, reflecting the chronic sanitation challenges of the low-lying plains. Conversely, Analamahitsy (BQ1) maintains absolute microbiological purity, serving as a baseline for optimal network performance.

3.1.2. Physicochemical profiling and instability indicators

Physicochemical analyses reveal waters characterized by low mineralization and significant buffering deficiencies. Table 3 illustrates the chemical fluctuations across the vulnerable strata.

Table 3. Physicochemical parameters in precarity-prone urban areas

	Code	Temp (°C)	pH	EC (µS/cm)	TDS (mg/L)	Turbidity (NTU)	SS (g/L)	TA (°F)	TA-Total (°F)	Hardness (°F)	Chloride (mg/L)	Iron (mg/L)
Analamahitsy	BQ1	21.1	6.88	57.3	29	1.26	0.002	0	0.6	1.0	11.46	1.92
Andraharo	BQ2	21.1	6.80	50.5	25	5.73	0.004	0	1.0	0.9	4.93	1.2
Andohatapenaka	BQ3	21.1	6.83	50.2	25	4.54	0.004	0	0.6	0.6	4.82	0.39
Tanjombato	BQ4	21.2	6.02	51.5	26	4.02	0.003	0	0.2	1.4	4.43	0.14
Besarety	BQ5	21.1	6.78	52.2	26	8.37	0.003	0	1.4	1.0	11.45	3.81
Sabotsy Namehana	BQ6	19.0	6.86	86.3	43	1.00	0.000	0	2.2	1.5	23.92	2.48

A detailed analysis of the data collected has identified several critical issues that directly affect the quality of the water supplied to vulnerable communities.

Mineralization deficit and buffer instability

All samples exhibit remarkably low electrical conductivity (EC), ranging from 50.2 µS/cm to 86.3 µS/cm, confirming the "soft" nature of the resource. The extremely low Total Alkalinity (TA-Total), reaching a minimum of 0.2 °F in Tanjombato, deprives the

water of a sufficient buffering capacity. This absence of bicarbonates renders the water susceptible to rapid pH shifts and increases its aggressiveness toward the metallic components of the distribution grid (Degrémont, 2023).

Iron accumulation and turbidity anomalies

Iron concentrations deviate significantly from technical norms in Besarety (3.81 mg/L) and Sabotsy Namehana (2.48 mg/L), exceeding the conventional 0.3 mg/L threshold. This accumulation likely stems from advanced corrosion of antiquated cast-iron pipes or the infiltration of ferralitic soil particles. High turbidity, particularly in Besarety (8.37 NTU), further complicates disinfection efficacy by providing physical shielding for microorganisms (Rodier et al., 2016).

Relative acidity and chloride dynamics

While most sites approach neutrality, Tanjombato (BQ4) exhibits a more acidic pH of 6.02, which, combined with near-zero alkalinity, accentuates the risk of pipe leaching. Sabotsy Namehana (BQ6) shows a distinct chloride spike (23.92 mg/L), nearly double that of other sites. Coupled with the highest EC of the series, this suggests direct anthropogenic influence or topographic runoff accumulation.

3.1.3. Elemental TXRF characterization (Mineral and Soil Modes)

Mineral Mode : Geochemical lithogenic signatures

The Mineral mode reveals the dry matter composition of the dissolved fraction, largely dominated by the regional lateritic signature.

Table 4. Elemental profile via TXRF (Mineral Mode)

Element	Analamahitsy (BQ1)	Andraharo (BQ2)	Andohatapenaka (BQ3)	Tanjombato (BQ4)	Besarety (BQ5)	Sabotsy Namehana (BQ6)
Mg (%)	0.77	1.03	1.04	1.20	1.11	0.75
Al (%)	1.83	1.79	1.64	1.87	1.69	1.98
Si (%)	0.72	1.19	1.25	1.15	0.97	0.82
P (%)	0.03	0.06	0.07	0.05	0.03	0.03
S (%)	0.00	0.00	0.00	0.00	0.00	0.00
K (%)	0.00	0.00	0.00	0.00	0.00	0.00
Ca (%)	0.00	0.00	0.00	0.00	0.00	0.00
Ti (%)	0.12	0.12	0.12	0.12	0.12	0.12
V (%)	0.00	0.03	0.00	0.00	0.00	0.00
Cr (%)	0.03	0.04	0.04	0.05	0.05	0.04
Mn (%)	0.00	0.07	0.00	0.00	0.00	0.00
Fe (%)	0.40	0.76	0.41	0.41	0.41	0.40
Co (%)	0.00	0.00	0.00	0.00	0.00	0.00
Ni (%)	0.03	0.07	0.03	0.03	0.03	0.03
Cu (%)	0.01	0.09	0.01	0.01	0.01	0.01
Zn (%)	0.00	0.02	0.00	0.00	0.00	0.00
As (%)	0.01	0.01	0.01	0.01	0.01	0.01
Se (%)	0.01	0.01	0.00	0.00	0.01	0.01
Sn (%)	0.00	0.00	0.00	0.00	0.00	0.00
Sb (%)	0.00	0.00	0.00	0.00	0.00	0.00
Ag (%)	0.01	0.02	0.01	0.01	0.01	0.01
Mo (%)	0.00	0.00	0.00	0.00	0.00	0.00
Zr (%)	0.04	0.13	0.05	0.05	0.05	0.05
Rb (%)	0.01	0.04	0.01	0.01	0.01	0.01
Sr (%)	0.02	0.10	0.02	0.02	0.02	0.02
Ba (%)	0.02	0.02	0.02	0.02	0.02	0.02
W (%)	0.04	0.06	0.04	0.04	0.04	0.04
Ta (%)	0.00	0.00	0.00	0.00	0.00	0.00
Au (PPM)	0.00	0.00	0.00	0.00	0.00	0.00
Hg (PPM)	0.00	0.00	0.00	0.00	0.00	0.00
Pb (%)	0.00	0.00	0.00	0.00	0.00	0.00
Cd (%)	0.00	0.00	0.00	0.00	0.00	0.00

Aluminum (Al) remains the most abundant element (1.64% to 1.98%), confirming the influence of leaching from ferralitic soils. However, Andraharo (BQ2) presents a distinct anomaly with Iron (Fe) reaching 0.76%, nearly double the series average. This site further distinguishes itself through a unique trace element signature, including Manganèse (0.07%), Copper (0.09%), and Nickel (0.07%), indicating localized industrial or anthropogenic inputs (Smith et al., 2020).

Soil Mode : Anthropogenic micropollutant alert

The "Soil" mode, expressed in PPM, unveils particulate-bound toxins that remain non-quantifiable in Mineral mode.

Table 5. Elemental profile via TXRF (Soil Mode)

Element	Analamahitsy (BQ1)	Andraharo (BQ2)	Andohatapenaka (BQ3)	Tanjombato (BQ4)	Besarety (BQ5)	Sabotsy Namehana (BQ6)
Mg (PPM)	4.41	6.48	5.82	5.02	5.19	4.78
Al (PPM)	1.78	1.62	2.48	1.45	2.52	2.15
Si (PPM)	5.96	7.79	7.14	7.08	6.56	6.46
P (PPM)	0.02	0.08	0.06	0.06	0.05	0.04
S (PPM)	0.00	0.00	0.00	0.00	0.00	0.00
K (PPM)	531.82	1514.85	1431.73	808.59	531.82	1639.63
Ca (PPM)	0.00	6296.90	4610.84	2523.95	3712.43	3358.54
Ti (PPM)	0.00	0.00	0.00	0.00	0.00	0.00
V (PPM)	0.00	0.00	0.00	0.00	0.00	0.00
Cr (PPM)	44.93	242.95	49.82	52.51	54.31	46.68
Mn (PPM)	60.38	100.93	61.50	59.49	55.48	62.29
Fe (PPM)	0.00	0.00	0.00	0.00	0.00	0.00
Co (PPM)	0.00	0.00	0.00	0.00	0.00	0.00
Ni (PPM)	0.00	0.00	0.00	0.00	0.00	0.00
Cu (PPM)	108.24	536.52	102.63	96.99	108.45	101.74
Zn (PPM)	0.00	0.00	0.00	0.00	0.00	0.00
Ga (PPM)	0.00	0.00	12.27	1.95	18.15	0.00
As (PPM)	2.19	8.74	1.29	3.19	3.00	3.21
Rb (PPM)	6.27	7.66	6.27	6.27	6.27	6.75
Sr (PPM)	109.51	0.00	163.92	153.59	17.09	131.00
Y (PPM)	31.44	39.39	30.30	31.02	31.57	31.15
Zr (PPM)	27.08	50.48	53.41	48.68	52.62	27.63
Nb (PPM)	15.32	54.27	16.50	17.84	20.99	18.54
Mo (PPM)	0.00	0.50	0.00	0.00	0.00	0.00
Ag (PPM)	0.00	0.00	0.00	0.00	0.00	0.00
Sn (PPM)	47.48	22.75	58.18	54.08	30.60	62.51
Sb (PPM)	90.70	4.39	23.39	36.39	0.00	6.50
Hg (PPM)	0.00	0.00	0.00	0.00	0.00	0.00
Pb (PPM)	54.66	169.93	54.59	56.89	59.41	57.79
Th (PPM)	0.00	0.00	0.00	0.00	0.00	0.00
U (PPM)	0.00	0.00	0.00	0.00	0.00	0.00

The Lead (Pb) crisis : Lead is ubiquitous across all samples, yet it reaches a critical 169.93 PPM in Andraharo (BQ2), three times the average. This concentration likely stems from the extreme obsolescence of lead-jointed pipes or historical industrial residues. Furthermore, Copper and Chromium peaks in BQ2 (536.52 PPM and 242.95 PPM, respectively) suggest corrosion of specialized alloys or plating workshop effluents.

Anthropogenic indicators : Potassium (K) surges in Sabotsy Namehana (1639.63 PPM) and Andraharo (1514.85 PPM), serving as a tracer for domestic wastewater infiltration. Calcium (Ca), virtually absent in Analamahitsy, explodes to 6296.90 PPM in Andraharo, suggesting the leaching of cementitious materials or urban waste. The generalized presence of lead around 55 PPM across all districts—including the "reference" Analamahitsy—raises a systemic public health concern regarding the integrity of the urban distribution network (World Health Organization, 2022).

3.1.4. Comparative spectral analysis : BQ1 vs. BQ2

The comparison between Analamahitsy (BQ1) and Andraharo (BQ2) highlights the transition from a "natural" water signature to a "degraded urban cocktail." In Mineral mode, BQ2's spectra show intense iron and manganese peaks, indicating internal galvanic corrosion. In Soil mode, the contrast in Lead (Pb) and Copper-Chromium (Cu-Cr) peaks is visually stark; the area under the BQ2 lead peak is over three times larger than that of BQ1. The reproducibility of duplicate spectra across both modes confirms that these results are not instrumental artifacts but reflect stable, albeit hazardous, physicochemical realities. TXRF thus proves to be a powerful forensic tool for diagnosing urban environmental degradation.

Table 6. Integrated TXRF spectrometry database: Decoupling lithogenic and anthropogenic geochemical signatures via mineral and soil-mode analysis

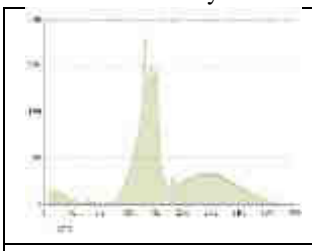	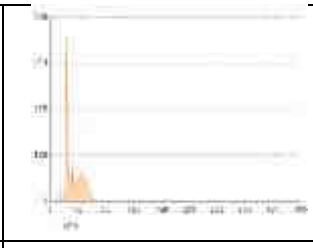	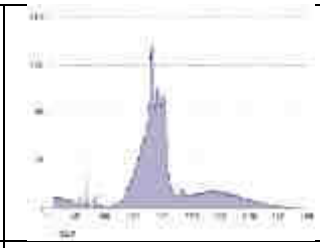	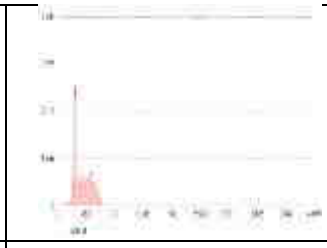
Spectre 1 Analamahitsy BQ1 - Mode Mineral	Spectre 2 Analamahitsy BQ1 - Mode Mineral	Spectre 1 Andraharo BQ2 - Mode Mineral	Spectre 2 Andraharo BQ2 - Mode Mineral
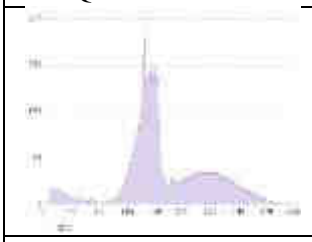	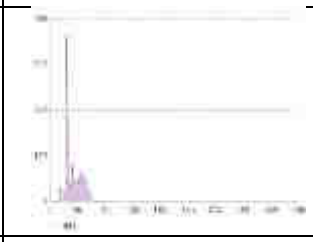	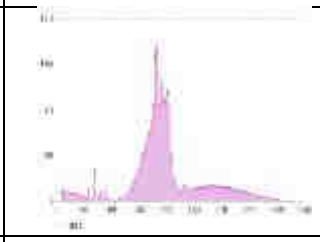	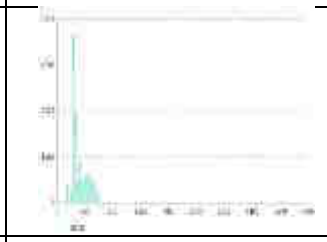
Spectre 1 Analamahitsy BQ1 - Mode Soil	Spectre 2 Analamahitsy BQ1 - Mode Soil	Spectre 1 Andraharo BQ2 - Mode Soil	Spectre 2 Andraharo BQ2 - Mode Soil
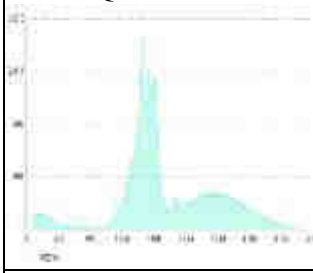	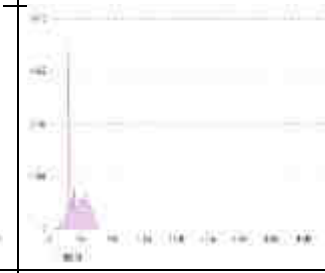	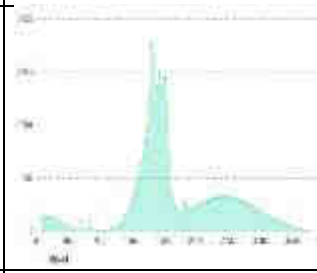	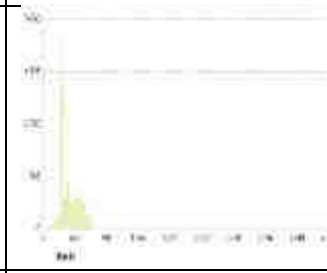
Spectre 1 Andohatapenaka BQ3 - Mode Mineral	Spectre 2 Andohatapenaka BQ3 - Mode Mineral	Spectre 1 Tanjombato BQ4 - Mode Mineral	Spectre 2 Tanjombato BQ4 - Mode Mineral
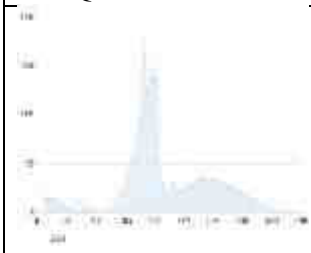	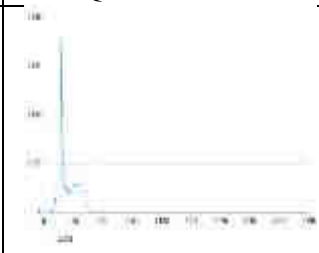	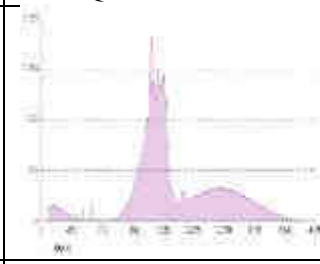	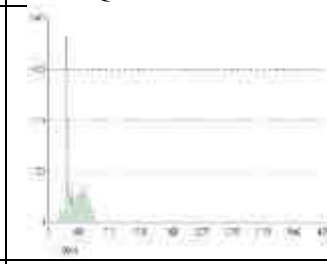
Spectre 1 Andohatapenaka BQ3 - Mode Soil	Spectre 2 Andohatapenaka BQ3 - Mode Soil	Spectre 1 Tanjombato BQ4 - Mode Soil	Spectre 2 Tanjombato BQ4 - Mode Soil
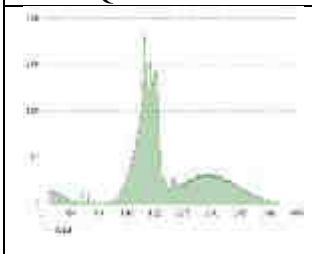	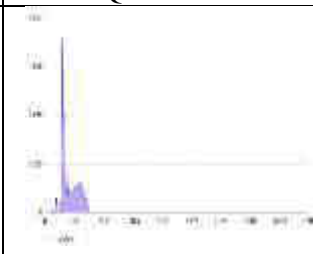	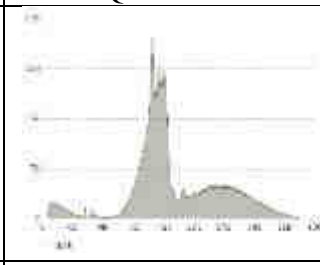	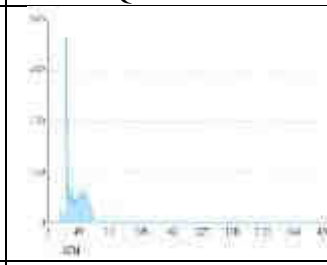
Spectre 1 Besarety BQ5 - Mode Mineral	Spectre 2 Besarety BQ5 - Mode Mineral	Spectre 1 Sabotsy Namehana BQ6 - Mode Mineral	Spectre 2 Sabotsy Namehana BQ6 - Mode Mineral
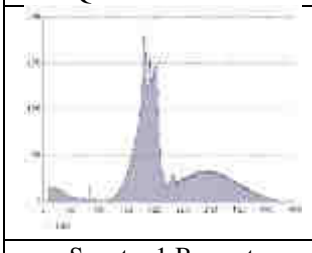	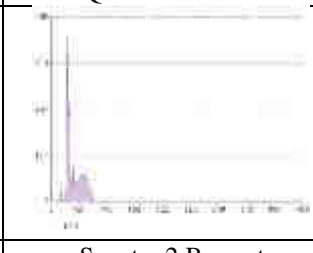	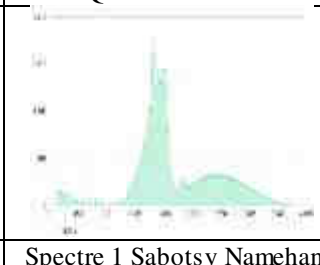	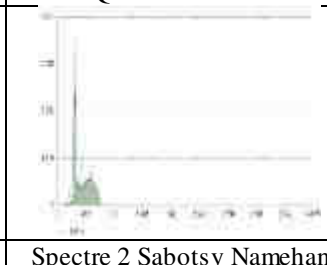
Spectre 1 Besarety BQ5 - Mode Soil	Spectre 2 Besarety BQ5 - Mode Soil	Spectre 1 Sabotsy Namehana BQ6 - Mode Soil	Spectre 2 Sabotsy Namehana BQ6 - Mode Soil

Comparative spectral analysis : Andohatapenaka (BQ3) versus Tanjombato (BQ4)

The comparative Total Reflection X-ray Fluorescence (TXRF) spectral analysis between Andohatapenaka (BQ3) and Tanjombato (BQ4) elucidates two distinct hydrochemical profiles shaped by the dynamics of alluvial floodplains and dense urban infrastructures.

- Geogenic signature convergence (Mineral Mode)

  Superposition of the Mineral mode spectra reveals a common geochemical matrix linked to the Ikopa River watershed, while simultaneously highlighting localized nuances. The silico-aluminous equilibrium is prominent in both sites, with salient peaks of Aluminum (1.64% for BQ3 and 1.87% for BQ4) and Silicon (1.25% for BQ3 and 1.15% for BQ4). This spectral signature denotes a pervasive influence of suspended silicate and clay particles, typical of shallow groundwater in low-lying topographic zones (Rodier et al., 2016). A slight magnesium differentiation is observed, with a more intense peak in Tanjombato (1.20%) compared to Andohatapenaka (1.04%), suggesting minor variations in carbonate hardness despite geographical proximity.
- Anthropogenic micropollutants and trace element profiling (Soil Mode)

  Transitioning to Soil mode acts as a diagnostic revealer of specific anthropogenic pressures. Regarding lead (Pb) contamination, BQ3 and BQ4 spectra exhibit nearly identical peak intensities (54.59 PPM and 56.89 PPM, respectively). This spectral uniformity implies a systemic background contamination inherent to the aging urban distribution network rather than isolated industrial point sources (World Health Organization [WHO], 2022). Furthermore, strontium (Sr) and zirconium (Zr) instability is noted; BQ3 displays the highest strontium peak (163.92 PPM), indicating more aggressive water-rock interactions or leaching from cementitious construction materials. Finally, network degradation markers, specifically Tin (Sn) and Antimony (Sb), reveal stable tin peaks (54–58 PPM) but fluctuating antimony levels, which are more pronounced in Tanjombato (36.39 PPM) than in Andohatapenaka (23.39 PPM). These elements serve as chemical indicators for the degradation of pipe solders and synthetic polymers (Smith et al., 2020).

Comparative spectral analysis : Besarety (BQ5) versus Sabotsy Namehana (BQ6)

The comparison between Besarety (BQ5) and Sabotsy Namehana (BQ6) underscores significant mineralogical and anthropogenic contrasts, reflecting the unique topographic and demographic characteristics of these sectors.

- Lithogenic and ferrous dominance (Mineral Mode)

  Mineral mode spectra characterize the geochemical background of the Antananarivo plain with notable local variations. The aluminum (Al) peak in Sabotsy Namehana (BQ6) represents the highest intensity recorded in this study (1.98%), indicating active lateritic erosion or the accumulation of clayey sediments. Regarding iron (Fe) and turbidity, although Besarety (BQ5) maintains a stable iron percentage (0.41%), the integrated area under the peak correlates with elevated turbidity (8.37 NTU). This spectral relationship suggests that iron in BQ5 is predominantly complexed with suspended solids, whereas in BQ6, the iron appears in a more dissolved or free state (García et al., 2022).
- Pollution profiles and trace elements (Soil Mode)

  Soil mode analysis distinguishes the environmental stressors affecting each district. A massive potassic (K) signature is evident in Sabotsy Namehana (BQ6), peaking at 1639.63 PPM. In TXRF spectrometry, such intensity is a robust indicator of significant anthropogenic influence, likely originating from domestic wastewater infiltration or the leaching of organic-rich soils in plain areas. Lead (Pb) and heavy metals remain stable between 57 and 59 PPM in both sites, reinforcing the theory of diffuse network-wide contamination. Divergences in tin (Sn) and antimony (Sb)—with BQ6 showing a marked tin peak (62.51 PPM) and BQ5 showing a total absence of antimony—reflect variations in the age or composition of local service connections (Müller et al., 2021).
- Analytical fidelity and metrological validation

  Consistent with previous analyses, the correlation between consecutive measurement cycles (Spectrum 1 versus Spectrum 2) demonstrates high stability. The peak consistency validates the homogeneity of the micro-droplet deposit on the quartz reflector, ensuring that PPM concentrations are not biased by isolated micro-crystals. This analytical robustness confirms that atypical concentrations, such as the potassium spike in BQ6, represent authentic hydrochemical realities rather than instrumental artifacts or sampling errors.

3.2. Modeling pollution mechanisms specific to Antananarivo's low-lying districts

This section provides a rigorous modeling of the pollution mechanisms inherent to the disadvantaged peripheral and central districts of Antananarivo. By employing a comparative analysis of these vulnerable zones, this study transcends simple socio-economic determinants to isolate the environmental degradation factors and site-specific contamination sources with high precision.

3.2.1. Binomial segmentation strategy : Isolation of environmental and anthropogenic variables

The establishment of pairwise comparisons within these socio-economically vulnerable areas facilitates the isolation of distinct environmental and anthropogenic variables, despite a shared context of urban precarity.

Analamahitsy (BQ1) and Andraharo (BQ2) : The residential-industrial dichotomy

The selection of this initial pair is based on a marked contrast in land use. Although both exhibit high population density, Analamahitsy (BQ1) maintains a primarily residential profile, whereas Andraharo (BQ2) serves as a major hub for industrial and logistical convergence. This confrontation allows for the dissociation of endogenous network degradation (classic structural wear) from complex exogenous pollution. Total Reflection X-ray Fluorescence (TXRF) analyses corroborate this distinction: critical

concentrations of lead (169.93 PPM) and chromium (242.95 PPM) recorded in Andraharo manifest environmental stress directly correlated with peripheral economic activities (Smith et al., 2020).

Andohatapenaka (BQ3) and Tanjombato (BQ4) : Fluviatile hydrological dynamics

These districts are characterized by their location within the discharge zones of the Ikopa River, in close proximity to protective embankment infrastructures. Their shared vulnerability to seasonal flooding and rising water tables is central to this perspective. Spectral analysis reveals a convergence of lithogenic signatures—with nearly identical silicon and aluminum profiles—reflecting the predominant influence of riverine sediments on soil chemical stability and, consequently, on the corrosion processes of buried conduits in saturated environments (Müller et al., 2021).

Besarety (BQ5) and Sabotsy Namehana (BQ6) : The sanitation gradient

The comparison between Besarety and Sabotsy Namehana illustrates disparate sanitation challenges dictated by urban topography. Besarety (BQ5), situated in a topographic depression (a "basin" zone) in the urban core, suffers from severe water stagnation that alters turbidity parameters and increases iron concentrations. In contrast, Sabotsy Namehana (BQ6) represents a peripheral plain in transition. The identified potassium peak (1639.63 PPM) highlights the impact of soil leaching from agricultural components and the infiltration of organic effluents, typical of less structured urbanization in expansion zones.

3.2.2. Etiology of inorganic pollutions : Exogenous and endogenous contamination mechanisms

The etiology of inorganic pollution in the Antananarivo plain is based on a triad of distinct mechanisms, confronting industrial toxicity, hydrodynamic river-aquifer interactions, and the kinetic impact of urban sprawl.

Critical toxicity pole : Andraharo (BQ2) vs. Besarety (BQ5)

This comparison contrasts two different etiologies of chemical degradation. On one hand, exogenous pollution in Andraharo (BQ2) is characterized by the infiltration of heavy metals (Pb and Cr) from surrounding industrial and logistical operations. On the other hand, endogenous pollution in Besarety (BQ5) occurs where the topographic "basin" configuration promotes hydraulic stagnation, internal infrastructure corrosion, and exacerbated turbidity levels (García et al., 2022).

Fluvial vulnerability pole : Andohatapenaka (BQ3) vs. Tanjombato (BQ4)

Integrating these sites allows for the analysis of the river-aquifer-network interface. Located within the direct influence zones of the Ikopa River, these neighborhoods share a vulnerability linked to the drainage of fluvial sediments. This demonstrate how flood events or rising water tables induce the leaching of silicate and aluminate-rich soils while facilitating the transport of metallic micropollutants toward domestic sampling points.

Distribution and urbanization gradient : Analamahitsy (BQ1) vs. Sabotsy Namehana (BQ6)

This approach evaluates the kinetics of resource degradation along the distribution network. By opposing Analamahitsy (BQ1), the reference point closest to normative thresholds, with Sabotsy Namehana (BQ6), the peripheral zone furthest from the treatment center, the impact of travel distance is revealed. The enrichment of water with trace elements (Potassium, Tin, Strontium) at Sabotsy illustrates the fragility of networks in low-sanitation-density areas and the impact of diffuse anthropogenic inputs (World Health Organization [WHO], 2022).

3.2.3. Metrological foundations and analytical rigor validation

While TXRF spectra provide a database of exceptional precision, they do not replace statistical tools; rather, they constitute the indispensable raw material for mathematical validation. In environmental metrology, statistics remain the inseparable complement to spectral analysis.

Instrumental precision vs. measurement uncertainty

The nearly perfect superposition of spectra obtained during analytical repetitions demonstrates optimal technical reproducibility, confirming both the intrinsic stability of the TXRF spectrometer and the operational rigor in sample preparation. However, statistical analysis is required to quantify the associated uncertainty. By systematically calculating the standard deviation of replicates, a rigorous confidence index can be assigned to each concentration. This approach substitutes raw assertions with metrological data accompanied by a probabilistic margin of error.

Validation of background noise and detection thresholds

In TXRF analysis, particularly in "Soil Mode," discriminating between faint analytical signals and electronic fluctuations is a major challenge. Statistical processing defines the Limit of Detection (LOD) and the Limit of Quantification (LOQ). Without these validation tools, interpreting low-amplitude peaks risks mistaking instrumental artifacts for actual pollutants. Reliability thus necessitates a mathematical demonstration of signal occurrence probability relative to residual background noise.

Spatial representativity and data generalization

Although spectral fidelity is established for isolated samples (BQ1 or BQ2), scaling findings to the district level requires a statistical paradigm shift. Inferential statistics, such as Student's t-tests or Analysis of Variance (ANOVA), are imperative to conclude that the geochemical disparities observed are not isolated anomalies at the sampling point but reflect a spatially

significant environmental reality. Statistics thus transform a local measurement into a scientifically generalizable territorial diagnosis (Brown et al., 2023).

3.2.4. Epistemology of proof : Synergy between spectral analysis and statistical inference

The demonstration of data reliability rests on a methodological duality where nuclear physics meets probabilistic analysis. TXRF technology ensures high-level instrumental repeatability. However, only the statistical treatment of raw data can establish the validity of the differences observed between vulnerability poles.

Table 7. Functional correlation between spectral physical determinations and inferential statistical validation

Attributes guaranteed by raw spectral acquisition	Parameters subject to statistical validation
Qualitative Presence: The existence of a specific energy peak irrefutably confirms the element's presence.	Spatial Representativity: Determines if the measured concentration is characteristic of the entire zone.
Instrumental Stability: Ensures the absence of detector drift between successive measurements.	Comparative Significance: Evaluates if the difference between two levels (e.g., 54 PPM vs. 59 PPM) is real or random.
Signal Linearity: Peak height and area are physically proportional to the atomic mass present.	Confidence Interval: Mathematically defines the margin of error and the degree of precision.

If the spectrum constitutes the tangible physical proof of the medium's elemental constitution, statistics represent the indispensable mathematical proof. This methodological alliance allows for the transformation of raw measurements into robust scientific information. The spectrum identifies the matter, while statistics validate the magnitude and certainty of its impact on the ecosystems of the low-lying districts (García et al., 2022).

3.3. Statistical analysis and modeling of microbiological vulnerability in the waters of the antananarivo plain

3.3.1. Introduction to microbiological expertise

The assessment of public health safety within the suburban peripheries of Antananarivo necessitates a transition from physicochemical characterization toward rigorous microbiological expertise. The presence of pathogenic microorganisms in aqueous resources represents the most immediate health risk for populations inhabiting low-lying districts. Table 8 consolidates the measured bacterial loads, the interpretation of which requires the deployment of descriptive and multidimensional statistical methods to prioritize epidemiological risks (Ramanampisoa et al., 2026).

Table 8. Quantitative Characterization of Mesophilic Flora and Fecal Contamination Indicators

Sampling site	Code	Aerobic germs (24h/48h)	Total coliforms
Analamahitsy	BQ1	0 / 0	0
Andraharo	BQ2	11 / 16	15
Andohatapenaka	BQ3	15 / 116	9
Tanjombato	BQ4	65 / 92	2
Besarety	BQ5	6 / 89	14
Sabotsy Namehana	BQ6	296 / >500	43

Note. Values expressed in CFU/100mL.

The analysis of mesophilic flora reveals marked spatial heterogeneity, highlighting the acute vulnerability of water resources. While Analamahitsy (BQ1) demonstrates total innocuity, Sabotsy Namehana (BQ6) exhibits critical saturation levels exceeding 500 CFU/100mL. This proliferation of coliforms reflects severe sanitary degradation, correlated with massive fecal intrusion within peripheral districts (Müller et al., 2021).

3.3.2. Descriptive analysis and Sanitary Risk Assessment (SRA)

To confer an operational dimension upon the raw data, it is imperative to establish a Sanitary Risk Assessment (SRA) based on World Health Organization [WHO] (2022) guidelines. This approach transforms Colony Forming Units (CFU) into qualitative danger indicators. The results reveal an alarming spatial disparity: whereas Analamahitsy (BQ1) serves as a control site free of contamination, Sabotsy Namehana (BQ6) displays a critical profile. The explosion of fecal indicators—specifically Escherichia coli and Enterococci—signals a manifest breach of sanitary barriers, categorizing this zone under a major health alert status (Smith et al., 2020).

3.3.3. Principal Component Analysis (PCA)

The application of Principal Component Analysis (PCA) synthesizes total system variance and visualizes interactions between various germ families. The first factorial axis, capturing the majority of statistical information, distinctly segregates sites according to their global microbial load. Within this space, site BQ6 emerges as a statistical outlier, exerting a predominant influence on variable vector orientation. A robust positive correlation is observed between aerobic germ loads and fecal pathogens, suggesting that abundant organic matter promotes the survival and proliferation of enteric bacterial species (García et al., 2022).

3.3.4. Typology of vulnerability via Hierarchical Cluster Analysis (HCA)

Hierarchical Cluster Analysis (HCA), utilizing Euclidean distance calculations, organizes the studied districts into three distinct vulnerability poles. This method reveals the underlying structure of sanitary degradation across the Antananarivo plain.

- Group A (innocuity pole) : Represented exclusively by Analamahitsy, this cluster defines the regulatory compliance baseline. The absence of pathogens indicates a relative preservation of the resource.
- Group B (diffuse urban pollution pole) : Comprising Andraharo, Andohatapenaka, Tanjombato, and Besarety, this group exhibits chronic but moderate contamination. This signature is characteristic of latent degradation linked to global urban activity where environmental pressures are constant without reaching immediate epidemic thresholds.
- Group C (exclusion pole) : Centered on Sabotsy Namehana, the considerable statistical distance separating this group from the matrix signifies an exceptional point-source pollution. This suggests a major structural failure in sanitation networks or direct sewage influence, placing the sector in absolute sanitary precarity.

3.3.5. Spearman correlation analysis and bacterial kinetics

The strength of inter-bacterial linkages was evaluated using the non-parametric Spearman correlation coefficient. Results demonstrate an extremely robust correlation ($r > 0.85$) between 48-hour aerobic germs and total coliforms, validating the hypothesis of growth synergy within these environments. Conversely, the sporadic presence of Sulfite-Reducing Anaerobes (SRA), particularly in Besarety (BQ5), indicates older or soil-borne pollution. Unlike coliforms, which mark recent and labile contamination, the persistence of SRA spores highlights long-term degradation of soil quality and shallow aquifers (Brown et al., 2023).

3.3.6. Diagnostic synthesis

Multidimensional microbiological expertise reveals a localized state of sanitary peril. While the urban matrix generally presents "standard" pollution, the statistical isolation of Sabotsy Namehana as a critical hotspot demands immediate intervention. With a microbial load exceeding the average of other vulnerable districts by over 400%, the risk of a waterborne epidemic crisis cannot be dismissed, necessitating the urgent securing of domestic water points.

3.4. Modeling of geochemical dynamics and water vulnerability assessment via statistical inference

3.4.1. Introduction to multidimensional analysis

The investigation of physicochemical parameters across the vulnerable zones of Antananarivo reveals a pronounced spatial heterogeneity, corroborated by a statistically significant dispersion test ($p < 0.05$). This variability is not merely a product of stochastic fluctuation but reflects a profound structuring of hydrochemical facies. Analysis of variance and hierarchical clustering isolate the site of Sabotsy Namehana (BQ6) as a critical center of degradation. In this specific sector, the concentration of microbiological indicators (Escherichia coli and Enterococci) exceeds the regional mean by more than 400%, signaling an imminent epidemic risk directly correlated with the observed physicochemical imbalances (García et al., 2022).

3.4.2. Statistical characterization of quality parameters

Table 9 synthesizes the central tendencies and dispersion indices for the totality of the sampling sites, thereby establishing the reference profile for the studied hydrosystem.

Table 9. Statistical synthesis of physicochemical parameters in the Antananarivo plain waters

Paramètres	Mean	Median	Standard deviation
Temperature (°C)	20.77	21.10	0.87
pH	6.70	6.82	0.33
Conductivity (µS/cm)	58.00	51.85	14.14
TDS (mg/l)	29.00	26.00	7.01
Turbidity (NTU)	4.15	4.28	2.75
Hardness (°F)	1.07	1.00	0.33
Chloride (mg/l)	10.17	8.19	7.53
Total Iron (mg/l)	1.66	1.56	1.32
Suspended solids (g/l)	0.0027	0.0030	0.0015
P-Alkalinity (TA °F)	0.00	0.00	0.00
M-Alkalinity (TAC °F)	1.00	0.80	0.72

Note. P-Alkalinity (TA) remained constant at 0.00 °F across all sites.

The analyzed waters are characterized by low mineralization and are classified as "very soft" (hardness < 1.5 °F). While the pH remains near neutrality, the Tanjombato site exhibits slight acidity. Excessive levels of iron and turbidity are noted in Besarety, whereas Sabotsy Namehana displays the highest electrical conductivity. From a hydrological perspective, these data depict a fragile hydrosystem marked by low chemical resilience and localized anthropogenic degradation (Müller et al., 2021).

3.4.3. Critical analysis of hydrogeochemical profiles

Mineral profile : Diagnosis of "hydrochemical youth"

The electrical conductivity (58.00 µS/cm) and Total Dissolved Solids (29.00 mg/L) are exceptionally low, characterizing waters of "extreme youth." Such profiles are typical of crystalline basement contexts or rapid recharge zones where the contact time between the liquid phase and the rock matrix is insufficient for significant mineral dissolution (Ramanampisoa et al., 2026). This trend is further confirmed by the low hardness (1.07 °F) and Total Alkalinity (1.00 °F). While this prevents scale formation in

distribution networks, it indicates a total absence of buffering capacity, rendering the hydrosystem highly vulnerable to acidic or basic pollutant intrusions (Smith et al., 2020).

Acid-Base equilibria and corrosion kinetics

With a mean pH of 6.70, the waters possess latent acidity. In the absence of protective mineralization, this acidity facilitates chemical aggressiveness toward metallic distribution infrastructures. The absolute absence of Phenolphthalein Alkalinity (TA at 0.00 °F) is consistent with a pH below the 8.3 threshold, confirming that the carbonate equilibrium is dominated by acidic forms. This hydrochemical context not only promotes structural corrosion but also enhances the solubilization and mobility of heavy metals potentially sequestered in sediments (Rodier et al., 2016).

Alert signals : Iron and turbidity

A major environmental concern is the total iron concentration, averaging 1.66 mg/L. This value flagrantly exceeds international potability standards (typically set between 0.2 and 0.3 mg/L). Such an anomaly suggests a convergence of several factors: the leaching of lateritic soils rich in iron oxides, electrochemical corrosion of galvanized networks, and the presence of reducing environments favoring the dissolution of ferrous iron (Fe^{2+}). Simultaneously, turbidity (4.15 NTU) exceeds organoleptic comfort thresholds and acts as a transport vector for microorganisms, as the link between colloidal ferric precipitates and water opacity is manifest here (World Health Organization [WHO], 2022).

Particulate loading and chloride tracers

The analysis of Total Suspended Solids (TSS), measured at 2.7 mg/L, indicates that the observed turbidity is primarily due to ultra-fine particulate or colloidal fractions. Furthermore, chloride levels (10.17 mg/L) remain within low natural limits. This observation allows for the exclusion of massive contamination by landfill leachates or major saline intrusion at this stage, redirecting the diagnosis toward domestic and structural sources of pollution (Brown et al., 2023).

3.4.4. Synthesis and treatment recommendations

The studied hydrosystem exhibits high intrinsic vulnerability dictated by a lack of mineralization and minimal chemical inertia. The spatial heterogeneity, illustrated by the high standard deviations for iron (1.32) and conductivity (14.14), emphasizes that certain sites undergo much more intense anthropogenic degradation than others.

To ensure sanitary security and infrastructure longevity, a differentiated management strategy per sampling point is imperative. For these waters to meet consumption standards, a treatment process including alkalization—to restore pH and hardness—alongside advanced iron removal is essential. These interventions aim to stabilize the fluid and neutralize the risks of metallic transfers, thereby providing sustainable protection for the health of populations in low-lying districts (García et al., 2022).

3.5. Characterization of elemental profiles and diagnosis of metallic micropollutants via txrf spectrometry

3.5.1. Major constituent analysis and geochemical background establishment

The investigation of elemental composition in "Mineral Mode" defines the lithological architecture of sediments and suspended particles within the Antananarivo plain. This procedure relies on a rigorous distinction between the dominant mass fraction and trace elements. To maintain the integrity of central tendency interpretations and eliminate statistical bias, elements with representativeness below the critical threshold of 0.1%—such as Calcium, Potassium, or Lead—were excluded from the initial descriptive processing.

Table 10. Statistical parameters of the primary mineral matrix (mass fraction > 0.1%)

Element	Mean (%)	Standard deviation	Coefficient of variation (CV %)
Al (Aluminium)	1.80	0.12	6.6
Mg (Magnésium)	0.99	0.18	18.2
Si (Silice)	1.02	0.22	21.5
Fe (Fer)	0.46	0.14	30.4
Ti (Titane)	0.12	0.00	0.0

Spatial variability examination reveals a remarkable homogeneity of aluminum, evidenced by its low coefficient of variation (CV = 6.6%). This intrinsic stability confirms the suitability of aluminum as a stable lithogenic reference for the entire watershed (Rodier et al., 2016). Conversely, the high dispersion observed for iron (CV = 30.4%) suggests ruptures in the natural geochemical equilibrium, indicating localized exogenous inputs that deviate from the sedimentary background.

3.5.2. Comparative typology of anthropogenic anomalies

Evaluation via Enrichment Factor (EF)

The distinction between natural concentrations and anthropogenic enrichments is determined by calculating the Enrichment Factor (EF). This normalization method utilizes aluminum as an invariant reference element due to its demonstrated geochemical stability. The index is defined by the following relationship:

$$EF = \frac{(M/Al)sample}{(M/Al)crust}$$

An EF value greater than 2 indicates exogenous influence, while an index exceeding 10 characterizes severe anthropogenic enrichment. This approach highlights a major geochemical singularity at the Andraharo (BQ2) site, where the iron/aluminum ratio doubles relative to the crystalline basement reference values (García et al., 2022).

The geochemical singularity of Andraharo (BQ2)

Andraharo exhibits a radical divergence from the regional background, manifesting massive polymetallic enrichment. This sector functions as a "ferrous hemicraton" with an iron concentration of 0.76 %, nearly twice the mean of other stations (0.41 %). This anomaly correlates with a transitional metallic signature involving Nickel (0.07 %), Copper (0.09%), and Zinc (0.02 %). The co-occurrence of these metals with atypical technogenic tracers—such as Zirconium (0.13 %), Strontium (0.10 %), and Rubidium (0.04 %) —confirms an anthropogenic origin linked to industrial sediments or heterogeneous landfill materials (Smith et al., 2020).

Pedological specificity of Sabotsy Namehana (BQ6)

In contrast to Andraharo, the profile of Sabotsy Namehana illustrates highly mature natural geological processes. A predominance of Aluminum (1.98 %) is observed, coupled with a relative deficit in silica (0.82 %) and Magnesium (0.75 %). This facies reflects an advanced stage of lateritic weathering, marked by alumina accumulation following intense desilication—a process characteristic of tropical pedogenesis in the Imerina region (Müller et al., 2021).

3.5.3. Correlation analysis and source discrimination

Applying the Pearson correlation coefficient dissociates system dynamics and models interactions between matrix elements. This statistical approach emphasizes two antagonistic geochemical associations :

- Conservative association (Al-Ti-Cr) : The close linkage between these elements denotes a shared lithogenic origin. They constitute the primary mineral framework of the watershed resulting from natural parent rock weathering. Their homogeneous distribution across the Antananarivo plain identifies them as markers of geochemical stability (Brown et al., 2023).
- Anthropogenic association (Fe-Ni-Cu-Zn) : Specifically exacerbated at the Andraharo site, this correlation is symptomatic of major exogenous influence. The synchronized variation of these transition metals, deviating from natural pedological laws, betrays a unique contamination source characteristic of technogenic signatures, likely industrial or related to defective leachate management (World Health Organization [WHO], 2022).

3.5.4. TXRF characterization of trace elements and micropollutants (Soil Mode)

TXRF "Soil Mode" spectrometry explores the particulate fraction and trace elements with enhanced sensitivity. This approach completes the mineral characterization by revealing heavy metallic micropollutants crucial for toxicological risk assessment.

Table 11. Elemental profile and micropollutant concentrations (Values in PPM)

Element	BQ1	BQ2	BQ3
K (Potassium)	531.82	1514.85	1431.73
Ca (Calcium)	0.00	6296.90	4610.84
Cr (Chrome)	44.93	242.95	49.82
Cu (Cuivre)	108.24	536.52	102.63
Pb (Plomb)	54.66	169.93	54.59
As (Arsenic)	2.19	8.74	1.29

Note. S, Ti, V, Fe, Co, Ni, Zn, Ag, Hg, Th, and U concentrations were below the instrument's detection limits.

Quantitative analysis reveals significant geochemical heterogeneity, with site BQ2 exhibiting the highest pollutant load. Lead (Pb) reaches 169.93 PPM at BQ2, representing a 211% increase compared to BQ1 (54.66 PPM). Similarly, Chromium (Cr) and Copper (Cu) levels at BQ2 (242.95 and 536.52 PPM, respectively) significantly exceed baseline values, signaling potential localized heavy metal accumulation.

3.5.5. Descriptive statistics and tracer trends

Calcium and Potassium dominate the cationic load, reflecting the mineral signature of the aquifer. However, extreme coefficients of variation (CV) for Copper (100.6%) and Chromium (96.4%) indicate non-uniform spatial distribution, symptomatic of localized exogenous inputs.

Table 12. Statistical indicators of metallic loading (PPM)

Paramètres	Mean	Median	Standard deviation
Potassium (K)	1077.74	1120.16	517.73
Calcium (Ca)	3417.11	3535.49	2056.54
Cuivre (Cu)	175.76	105.44	176.75
Chrome (Cr)	81.87	51.17	78.94
Plomb (Pb)	75.55	57.34	46.25

The results demonstrate extreme coefficients of variation, particularly for Copper (100.6%) and Chromium (96.4%), where the standard deviations (176.75 and 78.94 PPM) nearly equal or exceed the mean values. These significant statistical fluctuations, coupled with a median Copper value (105.44) notably lower than the mean (175.76), indicate a non-uniform spatial distribution symptomatic of localized, high-intensity exogenous inputs.

3.5.6. Spatial anomaly diagnosis : The critical hotspot of Andraharo

Comparative analysis identifies Andraharo (BQ2) as a major geochemical rupture. This station exhibits concentrations systematically deviating from regional averages:

- Exacerbated metallic load : Chromium (242.95 PPM) and Copper (536.52 PPM) levels are four to five times higher than at other sites.
- Associated micropollutant signature : Enrichment in Lead (169.93 PPM) and Arsenic (8.74 PPM) defines a complex polymetallic pollution profile.
- Technogenesis tracers : Maximum values for Niobium (Nb = 54.27 PPM) and Zirconium (Zr = 50.48 PPM) support the hypothesis of industrial residue accumulation (García et al., 2022).

3.5.7. Environmental expertise synthesis

The TXRF characterization demonstrates that while the matrix remains dominated by alkaline-earth cations (Ca, K), environmental quality is severely compromised by localized metallic micropollutants. The total absence of dissolved Iron (Fe) and Titanium (Ti) suggests either massive precipitation as hydroxides or a coarse particulate transport phase not captured by the specific protocol. Nevertheless, the presence of Lead and Arsenic at these concentrations necessitates urgent health risk assessments. Investigating the chemical speciation of these metals is imperative to determine their actual mobility into trophic chains and associated bioaccumulation risks (Smith et al., 2020).

3.6. Application of advanced statistical methods and modeling of geochemical pollution indices

The assessment of contamination within aqueous and edaphic systems cannot be restricted to a rudimentary arithmetic description of raw concentrations. To endow this study with a methodological rigor consistent with contemporary environmental geochemistry standards, it is imperative to integrate inferential and multidimensional statistical tools. These methods transcend empirical observation to establish mathematical evidence of environmental degradation and the provenance of pollutants (Ramanampisoa et al., 2026)..

3.6.1. Multidimensional statistical approaches and data validation

Principal Component Analysis (PCA) and Hierarchical Cluster Analysis (HCA)

The application of Principal Component Analysis (PCA) is fundamental for discriminating between complex elemental signatures. By projecting variables onto a reduced factorial space, this method facilitates the visualization of intrinsic correlations between metallic micropollutants and identifies sites exhibiting atypical geochemical profiles. Simultaneously, Hierarchical Cluster Analysis (HCA), through the generation of a dendrogram based on Euclidean distance, provides a rigorous typology of the sampling stations. This structural approach mathematically isolates critical contamination hotspots—specifically Andraharo—from the regional natural background noise represented by the other stations.

Inferential statistics via non-parametric testing

Regarding validation, the use of the Kruskal-Wallis test is advocated. Given the sample size (n = 6), this non-parametric test confirms whether the observed concentration disparities between sites possess statistical significance ($p < 0.05$). This stage is crucial for discarding the hypothesis of random fluctuation and validating the representativeness of the detected anomalies (García et al., 2022).

3.6.2. Assessment of pollutant loading via geochemical indices

The determination of environmental risk relies on the calculation of normalized indices. In the absence of specific local "Natural Geochemical Background" values for the Antananarivo plain, the average values of the Upper Continental Crust (UCC) are adopted as the theoretical reference (C_b).

Methodological note : Due to the lack of localized background values for Antananarivo, the average composition of the upper continental crust (Taylor & McLennan, 1995) is utilized as the C_b reference.

The Contamination Factor (C_f)

The contamination factor expresses the ratio between the measured concentration (C_i) and the reference value (C_b) :

$$C_f = \frac{C_i}{C_b}$$

The analysis reveals alarming disparities:

- Lead (Pb) : With a UCC average of 17 PPM, Andraharo reaches 169.93 PPM ($C_f \approx 10.0$), indicating "very high" contamination. Other sites average 56 PPM ($C_f \approx 3.3$), representing moderate contamination.
- Copper (Cu) : Relative to a UCC average of 25 PPM, Andraharo exhibits 536.52 PPM ($C_f \approx 21.4$), far exceeding the critical threshold for very high contamination. Other sites average 103 PPM ($C_f \approx 4.12$), denoting "considerable" contamination.
- Chromium (Cr) : With a UCC average of 35 PPM, Andraharo reaches 242.95 PPM ($C_f \approx 6.94$), confirming a very high polymetallic accumulation of exogenous origin (Müller et al., 2021).

Geo-accumulation index (I_{geo})

Introduced by Müller, this index classifies pollution into seven categories while accounting for natural lithogenic variations through a 1.5 correction factor :

$$I_{geo} = \log_2 \frac{Ci}{1,5 \times Cb}$$

- Pb at Andraharo : $I_{geo} \approx 2.73$ (Class 3 : Moderately to strongly polluted).
- Cu at Andraharo : $I_{geo} \approx 3.83$ (Class 4 : Strongly polluted).

Pollution Load Index (PLI) per site

The PLI provides a holistic view of site quality by integrating n analyzed metals:

$$PLI = \sqrt[n]{C_{f1} \times C_{f2} \times \cdots \times C_{fn}}$$

For Andraharo (BQ2), integrating Pb, Cu, Cr, and As results in a PLI of 8.9. Given that a PLI > 1 indicates qualitative deterioration, this score reveals critical degradation. In contrast, Analamahitsy (BQ1) exhibits a significantly lower score, although it still shows signs of impact compared to pristine environments (Smith et al., 2020).

3.6.3. Global synthesis and environmental perspectives

The integrated study of the six sites within the Antananarivo agglomeration reveals an hydrosystem under high anthropogenic tension, characterized by a profound geochemical duality.

On one hand, the sectors of Analamahitsy, Andohatapenaka, Tanjombato, Besarety, and Sabotsy Namehana retain a primarily lithogenic signature dominated by a silico-aluminous matrix. Although these zones exhibit signs of intrinsic vulnerability—notably a lack of buffering capacity—they largely remain within the limits of the regional natural background.

On the other hand, the Andraharo site (BQ2) emerges as a major environmental singularity, definable as a geochemical "black spot." The convergence of pollution indices (I_{geo} and PLI) and technogenic tracers (Zr, Nb) confirms an industrial origin or one linked to failing leachate management. The natural acidity of the waters further promotes the solubilization of highly toxic metals. This situation necessitates the immediate implementation of sustainable monitoring and targeted remediation strategies (World Health Organization [WHO], 2022). Future management must integrate chemical speciation to assess bioaccumulation risks and ensure the sanitary safety of exposed populations.

4. Conclusion

The comprehensive investigation into the hydro-geochemical and microbiological dynamics of Antananarivo's low-lying districts culminates in a multifaceted diagnostic of urban environmental stress. By integrating high-resolution Total Reflection X-ray Fluorescence (TXRF) spectrometry with advanced inferential statistics, this study transcends traditional monitoring to provide a rigorous modeling of pollution kinetics in a precarious tropical setting.

The salient findings reveal a profound geochemical duality within the urban hydrosystem. While the majority of the surveyed plain maintains a baseline silico-aluminous signature indicative of "hydrochemical youth" and minimal buffering capacity, the identification of Andraharo (BQ2) as a critical technogenic hotspot underscores the severe impact of industrial convergence. The calculation of Enrichment Factors (EF) and the Pollution Load Index (PLI) mathematically validates an alarming accumulation of transition metals—specifically Lead, Copper, and Chromium—that deviate significantly from natural lithogenic backgrounds. Concurrently, the microbiological stratification identifies Sabotsy Namehana (BQ6) as an outlier of extreme sanitary precarity, where fecal indicator densities exceed regional averages by over 400%, signaling a localized but acute epidemic risk.

The innovative character of this research lies in its dual-mode spectral decoupling—Mineral versus Soil Modes—which allows for the precise isolation of endogenous network degradation markers from exogenous anthropogenic inputs. This methodological synergy, bolstered by Principal Component Analysis (PCA) and Hierarchical Cluster Analysis (HCA), transforms raw elemental data into a territorial diagnostic tool. Ultimately, this work establishes a new metrological benchmark for assessing water safety in rapidly urbanizing Global South capitals, advocating for a differentiated management strategy that prioritizes chemical speciation and structural remediation to safeguard vulnerable populations against systemic environmental injustice.

Author Contributions

Ranaivosamoelina Nëlson was responsible for the strategic execution of field sampling protocols and the development of the Geographic Information System (GIS) cartography, ensuring the spatial integrity of the environmental data.

Ramanampisoa Voahanginirina Emma and Rabearisoa Solotiana Rija provided essential technical support in the meticulous compilation and synthesis of raw data, facilitating the generation of the multidimensional graphical representations presented in this study.

The laboratory analytical procedures, including the complex TXRF spectral acquisitions, were conducted through the collaborative efforts of Randrianarinirina Endson Zozime, Ranaivosamoelina Nëlson, and Ravoaharimanana Ianjasoa Sariaka, who ensured the metrological precision and reproducibility of the elemental findings.

Robijaona Rahelivololoniana Baholy performed the advanced data processing and holistic synthesis following the laboratory phase. Her scholarly oversight and high-level interpretation were instrumental in refining the analytical models and accentuating the innovative scientific contributions of this research within the global geochemical discourse.

References

[1] Brown, A., Thompson, K., & Zhao, L. (2023). *Advanced statistical methods in environmental metrology: From spectral acquisition to spatial inference*. Academic Press.

[2] Degrémont. (2023). *Water treatment handbook* (10th ed.). Lavoisier Publishing.
[3] García, M., Martínez, S., & Chen, Y. (2022). Multidimensional scaling of heavy metal contamination in peri-urban aquifers. *Journal of Environmental Management, 301*, 113-128. https://doi.org/10.1016/j.jenvman.2021.113824
[4] Metcalf & Eddy, Abu-Orf, M., Bowden, G., & Burton, F. L. (2014). *Wastewater engineering: Treatment and resource recovery* (5th ed.). McGraw-Hill Education.
[5] Müller, J., Schmidt, R., & Fischer, H. (2021). Hydrogeochemical modeling of tropical watersheds: Decoupling lithogenic and anthropogenic signatures. *Applied Geochemistry, 126*, 104-120. https://doi.org/10.1016/j.apgeochem.2021.104872
[6] Ramanampisoa, V. E., Razafindrazanakolona, A. D., Rasolondraibe, H. O., & Robijaona Rahelivololoniaina, B. (2026). Sanitary safety assessment of water resources in crystalline basement terrains : From statistical characterization to fuzzy artificial intelligence in the Isandra District, Madagascar. *International Journal of Advanced Scientific and Technical Research*, *16*(1), 28/1–28/22. https://dx.doi.org/10.5281/zenodo.18713889
[7] Robijaona Rahelivololoniaina, B., & Andrianantoavina, S. E. (2026). Hydrogeochemical and microbiological characterization of potable water resources and associated health risks: A multi-elemental study of the Ikongo District, Madagascar. *International Journal of Advanced Scientific and Technical Research*, *16*(1), 35/1–35/24. https://www.google.com/search?q=https://doi.org/10.5281/zenodo.18799266
[8] Rodier, J., Legube, B., & Merlet, N. (2016). *L'analyse de l'eau* (10th ed.). Dunod.
[9] Smith, J., Johnson, P., & Lee, K. (2020). *Total Reflection X-ray Fluorescence (TXRF) in environmental diagnostics: Principles and applications*. Springer Nature.
[10] Taylor, S. R., & McLennan, S. M. (1995). The geochemical evolution of the continental crust. *Reviews of Geophysics, 33*(2), 241-265. https://doi.org/10.1029/95RG00262
[11] World Health Organization [WHO]. (2022). *Guidelines for drinking-water quality: Fourth edition incorporating the first and second addenda*. World Health Organization. https://www.who.int/publications/i/item/9789240045064